Title

Altered Development of Amygdala-Connected Brain Regions in Males and Females with Autism

Journal

Journal of Neuroscience, 42(31)

ISSN

0270-6474

Authors

Lee, Joshua K

Andrews, Derek S

Ozturk, Arzu

et al.

Publication Date

2022-08-03

DOI

10.1523/jneurosci.0053-22.2022

Peer reviewed

Neurobiology of Disease

Altered Development of Amygdala-Connected Brain Regions in Males and Females with Autism

Joshua K. Lee,[1,2] Derek S. Andrews,[1,2] Arzu Ozturk,[3] Marjorie Solomon,[1,2] Sally Rogers,[1,2] David G. Amaral,[1,2*] and Christine Wu Nordahl[1,2*]

[1]MIND Institute, University of California Davis School of Medicine, Sacramento, California 95817, [2]Department of Psychiatry and Behavioral Sciences, and [3]Department of Radiology, University of California Davis School of Medicine, Sacramento, California 95817

Altered amygdala development is implicated in the neurobiology of autism, but little is known about the coordinated development of the brain regions directly connected with the amygdala. Here we investigated the volumetric development of an amygdala-connected network, defined as the set of brain regions with monosynaptic connections with the amygdala, in autism from early to middle childhood. A total of 950 longitudinal structural MRI scans were acquired from 282 children (93 female) with autism and 128 children with typical development (61 female) at up to four time points (mean ages: 39, 52, 64, and 137 months, respectively). Volumes from 32 amygdala-connected brain regions were examined using mixed effects multivariate distance matrix regression. The Social Responsiveness Scale-2 was administered to assess degree of autistic traits and social impairments. The amygdala-connected network exhibited persistent diagnostic differences (p values ≤ 0.03) that increased over time (p values ≤ 0.02). These differences were most prominent in autistics with more impacted social functioning at baseline. This pattern was not observed across regions without monosynaptic amygdala connection. We observed qualitative sex differences. In males, the bilateral subgenual anterior cingulate cortices were most affected, while in females the left fusiform and superior temporal gyri were most affected. In conclusion, (1) autism is associated with widespread alterations to the development of brain regions connected with the amygdala, which were associated with autistic social behaviors; and (2) autistic males and females exhibited different patterns of alterations, adding to a growing body of evidence of sex differences in the neurobiology of autism.

Key words: **amygdala; autism spectrum disorder; brain; development; longitudinal; sex difference**

Significance Statement

Global patterns of development across brain regions with monosynaptic connection to the amygdala differentiate autism from typical development, and are modulated by social functioning in early childhood. Alterations to brain regions within the amygdala-connected network differed in males and females with autism. Results also indicate larger volumetric differences in regions having monosynaptic connection with the amygdala than in regions without monosynaptic connection.

Introduction

Autism spectrum disorder (autism) is a heterogeneous neurodevelopmental condition that includes alterations to social-communication behaviors (Anon, 2013). While many cross-sectional MRI studies have investigated the neurobiology of autism, few studies have examined autistic brain development from early childhood onward. Moreover, much that we do know about the neurobiology of autism comes from studies with predominately male samples, and thus it remains unclear whether the neurologic bases of autism differ in females (Lai et al., 2015).

The amygdala acts as a central hub that coordinates subsystems broadly implicated in social functioning via its roles in regulating emotion, fear, anxiety, and affective valence (Amaral, 2002; Freese and Amaral, 2009; Rutishauser et al., 2013; Bickart et al., 2014; Mears and Pollard, 2016; Padmanabhan et al., 2017; Fadok et al., 2018; Hennessey et al., 2018). Thus, the amygdala

Received Jan. 7, 2022; revised Apr. 30, 2022; accepted June 8, 2022.

Author contributions: J.K.L., M.S., S.R., D.G.A., and C.W.N. designed research; J.K.L., D.S.A., A.O., and C.W.N. performed research; J.K.L. and C.W.N. analyzed data; J.K.L., D.G.A., and C.W.N. wrote the first draft of the paper; J.K.L., D.S.A., M.S., S.R., D.G.A., and C.W.N. edited the paper; J.K.L. wrote the paper.

This work was supported by National Institute of Mental Health R01MH104438, R01MH103284, and R01MH103371; UC Davis MIND Institute Intellectual and Developmental Disabilities Research Center P50HD103526; and Autism Center of Excellence P50HD093079. This work was also supported in part by the Health Resources and Services Administration of the U.S. Department of Health and Human Services under the Autism Intervention Research Network on Physical Health Grant UT2MC39440. The information, content and/or conclusions are those of the authors and should not be construed as the official position or policy of, nor should any endorsements be inferred by Health Resources and Services Administration, Department of Health and Human Services or the U.S. Government.

*D.G.A. and C.W.N. contributed equally to this work as co-senior authors.

D.G.A. is on the Scientific Advisory Boards of Stemina Biomarkers Discovery, Inc. and Axial Therapeutics. The remaining authors declare no competing financial interests.

Correspondence should be addressed to Joshua K. Lee at jkilee@ucdavis.edu.

https://doi.org/10.1523/JNEUROSCI.0053-22.2022

has long been the focus of studies investigating the neurobiological bases of autism (Munson et al., 2006; Schumann and Amaral, 2006; Mosconi et al., 2009; Bickart et al., 2014; Hennessey et al., 2018; Müller and Fishman, 2018; Mundy, 2018; Gangopadhyay et al., 2021). Converging evidence suggests that the amygdala undergoes a period of accelerated volumetric growth in autism that ends at some point in childhood (Schumann et al., 2004; Nordahl et al., 2012; Morgan et al., 2014; Avino et al., 2018; Xu et al., 2020; Shen et al., 2022). For example, enlargement of the amygdala has been observed in young children with autism (Schumann et al., 2004, 2009; Schumann and Amaral, 2006; Mosconi et al., 2009; Nordahl et al., 2012), and postmortem research has reported increased numbers of amygdala neurons in autistic children and adolescents, but not autistic adults (Avino et al., 2018). The amygdala also exhibits robust sex differences in typically developing individuals (Ritchie et al., 2018), differences that may be diminished in autism (Lee et al., 2020a). Together, these factors make the amygdala an appealing target to explore autism neurophenotypes.

Functional connectivity studies of the amygdala, while useful, depend on correlative approaches that often link brain regions with no known synaptic pathway with the amygdala (Hori et al., 2020). Structural MRI studies, conversely, have tended to focus only on the amygdala in isolation. Here, we leveraged knowledge from neuroanatomical studies that have systematically mapped the afferent and efferent connections of the amygdala (Amaral and Price, 1984; Russchen et al., 1985; Insausti et al., 1987; Saunders et al., 1988; Carmichael and Price, 1995; Stefanacci et al., 1996; Stefanacci and Amaral, 2000, 2002; Amaral, 2002; Hori et al., 2020) to identify a set of brain regions with known monosynaptic anatomic connection to the amygdala. We then evaluated the anatomic volumes of these amygdala-connected brain regions to determine how their development may be altered in autism (see Fig. 1).

In this study, we characterized the volumetric development of this amygdala-connected anatomic network as a function of autism diagnosis, biological sex, and social functioning behaviors from early to middle childhood using multivariate distance matrix regression (MDMR) (Zapala and Schork, 2012). MDMR regresses a matrix representing how individuals differ across multiple measurements (e.g., the volumes of amygdala-connected brain regions) onto one or more predictors, accumulating evidence across multivariate outcomes. Complementing this approach, we examined effect sizes to determine which brain regions within the amygdala-connected profile contributed differences in the MDMR analysis (McArtor et al., 2017).

We predicted that the amygdala-connected network would exhibit global volumetric differences in association with autism diagnosis, sex, and age. We further predicted that development of the amygdala-connected network would proceed differently in autistic children than in nonautistic children. Finally, we predicted that the amygdala-connected network would differ across autistic males and females either quantitatively (magnitude of effect) or qualitatively (effects in different brain regions) (Bejerot et al., 2012; Werling and Geschwind, 2013; Hammill et al., 2021).

Materials and Methods

Participants. This longitudinal sample included a total of 950 scans from 282 participants with autism (93 female) and 132 nonautistic participants with typical development (TD) (61 female) enrolled in the UC Davis MIND Institute Autism Phenome Project and scanned up to 4 times, with three annual time points during early childhood (24-72 months of age; T1, T2, and T3, respectively) and a fourth time point during middle childhood (108-144 months of age; T4). Diagnosis of autism was performed using the Autism Diagnostic Interview–Revised and the Autism Diagnostic Observation Schedule (ADOS)-Generic or ADOS-2 by licensed, research-reliable clinical psychologists, and calibrated severity scores were computed (Lord et al., 1994, 2000, 2012; Gotham et al., 2009). A TD control group was screened for autism and developmental delay. TD controls were excluded if scores exceeded the clinical cutoff on the Social Communication Questionnaire ($\geq$11) (Rutter et al., 2003), if any subscale scores on the Mullen Scales of Early Learning developmental quotients (DQ) (Mullen, 1995) were 2 or more SDs below normative means, or if the individual had a first-degree relative with autism. All participants were English speaking and had no suspected vision, hearing, or neurologic conditions.

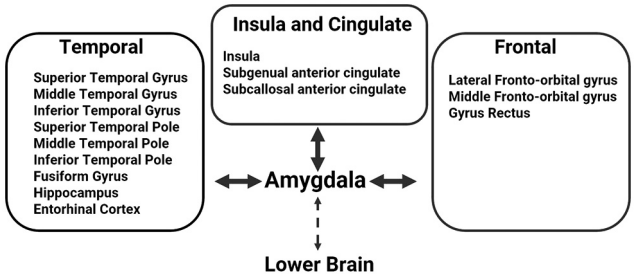

Figure 1. The amygdalocentric network comprised of temporal, cingulate, insula, and frontal gray matter regions. The listed regions share extensive monosynaptic afferent or efferent connection with the amygdala, providing in total 32 brain regions (16 regions × 2 hemispheres). Amygdala connections to lower brainstem nuclei were not assessed. The volumes of lower brainstem regions were not included in the current analysis.

The Social Responsiveness Scale-2 (SRS) (Constantino and Gruber, 2012) was administered to assess degree of autistic traits and social impairments. Total T scores at baseline T1 (mean age 38 months) were used to predict future volumetric trajectories in amygdala-connected anatomic networks in autistic children. An SRS T score of 75 is a widely used cutoff demarcating moderate from severe social impairments (Constantino and Gruber, 2012). We defined two groups of autistic children based on lower ($\leq$75, SRS$^-$, n = 136) and higher (>75, SRS$^+$, n = 78) T1 SRS T scores. Handedness was assessed using the Hand Preference Task at Time 1 (Spreen and Strauss, 1991).

All longitudinal research was conducted at the University of California Davis MIND Institute and Imaging Research Center and was approved by the UC Davis Institutional Review Board. Informed consent was obtained from a parent or legal guardian.

Imaging acquisition. Images were acquired during natural nocturnal sleep at T1 through T3 (Nordahl et al., 2008) or while awake at T4 using a behavioral analytic approach that improves compliance (Nordahl et al., 2016). All scans were acquired using a 3 Tesla Siemens Trio with an 8-channel head coil. At each session, a T1-weighted MPRAGE image was acquired to assess structural brain development (T1-T3: TR 2170 ms, TE 4.86 ms, FOV 256, 192 sagittal slices, 1.0 mm slice thickness, 8:46 acquisition time; T4: TR 2170 ms, TE 3.5 ms, FOV 256 mm, FA 7, 192 sagittal slices, 1.0 mm slice thickness; the latter sequence featuring a shorter acquisition [5:10] to increase compliance in awake scanning). All scans were acquired between January 2006 and February 2020. Uniform spatial measurement over time was achieved by imaging a calibration phantom at the end of each session and performing spatial distortion correction (ADNI MAGPHAM, Phantom Laboratory; Image Owl; http://www.imageowl.com) (Nordahl et al., 2012). Image quality control at acquisition was assessed both visually and with a previously described quantitative procedure (Nordahl et al., 2016). All structural scans were assessed by a pediatric neuroradiologist (A.O.) for clinically significant incidental brain findings.

Image processing. Images were defaced, identifiable information removed, and then uploaded to MRICloud for multi-atlas image segmentation (https://mricloud.org) (Mori et al., 2016). Segmentation entailed deforming an age-appropriate atlas of anatomically labeled structural images to a participant's MPRAGE using diffeomorphic registration (Nordahl et al., 2020; Reinhardt et al., 2020) producing a set of

Table 1. Sample characteristics[a]

		Boys		Girls	
		Autism	TD	Autism	TD
Participants		189	71	93	61
Participant scans included	Time 1	177	68	90	60
	Time 2	106	49	43	43
	Time 3	74	38	33	30
	Time 4	65	36	14	24
Participants with data from	Time 1 and Time 2	103	46	42	42
	Time 1 and Time 3	71	36	33	30
	Time 1 and Time 4	55	34	12	24
Age (mo)	Time 1	38.4 (6)	39.6 (6)	37.2 (6)	38.4 (7.2)
	Time 2	50.4 (6)	52.8 (7.2)	50.4 (6)	52.8 (6)
	Time 3	63.6 (4.8)	66 (6)	63.6 (6)	66 (6)
	Time 4	136.8 (12)	133.2 (9.6)	136.8 (8.4)	135.6 (9.6)
ADOS CSS	Time 1	7.44 (1.8)	—	7.37 (1.7)	—
SRS total scores	Time 1	70.7 (10.7)	—	72.6 (10.8)	—
DQ/IQ	Time 1	63.2 (21.3)	104.0 (12.0)	66.3 (22.8)	108.4 (11.7)

[a]Data are mean (SD).

candidate segmentations from which joint label fusion generates an optimal consensus segmentation (Ceritoglu et al., 2009; Tang et al., 2013; Wang and Yushkevich, 2013). Gray-matter anatomic labels were based on the LONI Probabilistic Brain Atlas (LPBA40) (Shattuck et al., 2008; Oishi et al., 2009). Outputted anatomic regions were visually inspected for slice-wise segmentation quality. Amygdala parcellations from this pipeline have been validated against gold-standard manual tracings within a subset of the current cohort (Nordahl et al., 2020).

Amygdala-connected network. We constructed a set of amygdala-connected brain regions, defined by selecting cortical ROIs from the MRICloud anatomic parcellations that have known monosynaptic connection with the amygdala (Amaral and Price, 1984; Russchen et al., 1985; Insausti et al., 1987; Saunders et al., 1988; Carmichael and Price, 1995; Stefanacci et al., 1996; Stefanacci and Amaral, 2000, 2002; Amaral, 2002; Hori et al., 2020). The volumes of each region (Fig. 1) were converted into proportions of the participant's concurrent total brain volume (TBV), accounting for overall brain size differences; the proportions of each brain regions were then standardized using z scores across participants to account for differences in size between brain regions.

Analytic strategy. MDMR is a multivariate method well suited for the analysis of high-dimensional MRI data (Zapala and Schork, 2012; Satterthwaite et al., 2015; Lee et al., 2020a). MDMR regresses a distance matrix onto an explanatory model (e.g., age, diagnosis) and residual error term (Gower, 1966; Zapala and Schork, 2012), and allows for the addition of a random effects term for mixed effects MDMR of longitudinal data. Distances are summary metrics that represent the overall dissimilarity between pairwise individuals across a network of outcome measures (e.g., a set of MRI measurements). Interpretation of MDMR results is aided though the use of distance-based redundancy analysis (dbRDA) to construct ordination plots, a constrained dimension-reduction technique for visualization (Legendre and Anderson, 1999; Anderson and Willis, 2003), and by estimating distances between group multivariate means using Euclidean projection (Apostol and Mnatsakanian, 2003). Since methods such as MDMR work on distances, they do not typically retain information about the individual outcomes that were used to construct the distance matrix. This limits the capacity to identify which outcomes had the strongest associations with a predictor. To overcome this limitation, we used a bootstrapping procedure to estimate the effect sizes for each outcome variable, providing vectors of effect sizes for each MDMR model parameter (i.e., effect sizes for each brain region) (McArtor et al., 2017; Lee et al., 2020a). Two vectors can be compared (e.g., effect sizes for each brain region in females and males) by computing their Dice similarity coefficient (DSC) (Dice, 1945), ranging from 0, indicating no agreement, to 1, indicating perfect agreement (i.e., identical patterns of effect sizes for each brain region). Outcomes of interest identified via effect size analysis were descriptively analyzed using univariate mixed effects models (Hoffman, 2015) with multiple fractionated polynomials (Long and Ryoo, 2010; for details, see Lee et al., 2020b). Simple effects tests were conducted by recentering variables to the age at T1, T2, T3, and T4 samples (~37, 50, 65, and 135 months, respectively) and reinspecting regression parameters. Multiple comparison corrections were performed using false discovery rate (FDR) (Benjamini and Hochberg, 1995).

Mixed MDMR analyses were conducted to assess differences in the volumetric development of the amygdala-connected network. A pairwise dissimilarity matrix was then computed using the Manhattan distance (Aggarwal et al., 2001). MDMR analyses were performed using models of the form: $Y = \beta_0 + \beta_1(\text{group}) + \beta_2(\text{age}) + \beta_3(\text{age}^2) + \beta_4(\text{group} \times \text{age}) + \beta_5(\text{group} \times \text{age}^2) + \beta_6(\text{sex})$, where group was autism diagnosis or SRS group. Sex differences were examined by adding constituent interactions and inspecting relevant parameters, and by comparing the effect sizes of individual regions in males and females.

Last, we tested the specificity of findings to the amygdala-connected network by (1) conducting MDMR analyses on 22 cortical gray matter regions that are not part of the amygdala-connected network (i.e., do not have monosynaptic connections with the amygdala), and (2) comparing effect sizes between the amygdala-connected network and cortical regions without monosynaptic connection with the amygdala. The cortical gray matter regions that were not part of the amygdala network comprised 22 left and 22 right hemispheric ROIs, including the inferior frontal gyri pars opercularis, orbitalis, and triangularis, the posterior, middle, and pole of the superior frontal gyri, the dorsal and posterior segments of the middle frontal gyri, the dorsal anterior and posterior cingulate, the precentral and postcentral gyri, the parahippocampal gyri the angular gyri, superior parietal gyri, the cuneus and precuneus, the lingual gyri, and the inferior, middle, and superior occipital gyri.

Data availability. Data described in the current research are available from the corresponding author on reasonable request.

Results

Sample characteristics

Table 1 reports sample characteristics. At T1, mean DQ was higher in TD children than autistic children ($B = 38$, $SE = 2.5$, $p \leq 0.00001$). Autistic males and females did not significantly differ on SRS Total T scores ($B = 1.8$, $SE = 1.6$, $p = 0.25$) or ADOS Calibrated Severity Scores ($B = 0.07$, $SE = 0.23$, $p = 0.75$), or DQ ($B = 3.1$, $SE = 2.8$, $p = 0.27$). The median SRS T scores of the autism SRS^- and SRS^+ groups were 64 and 80, respectively.

Development of the amygdala-connected anatomic network across diagnosis and sex

Autistic and TD children exhibited significant differences in amygdala-connected networks throughout childhood (diagnosis:

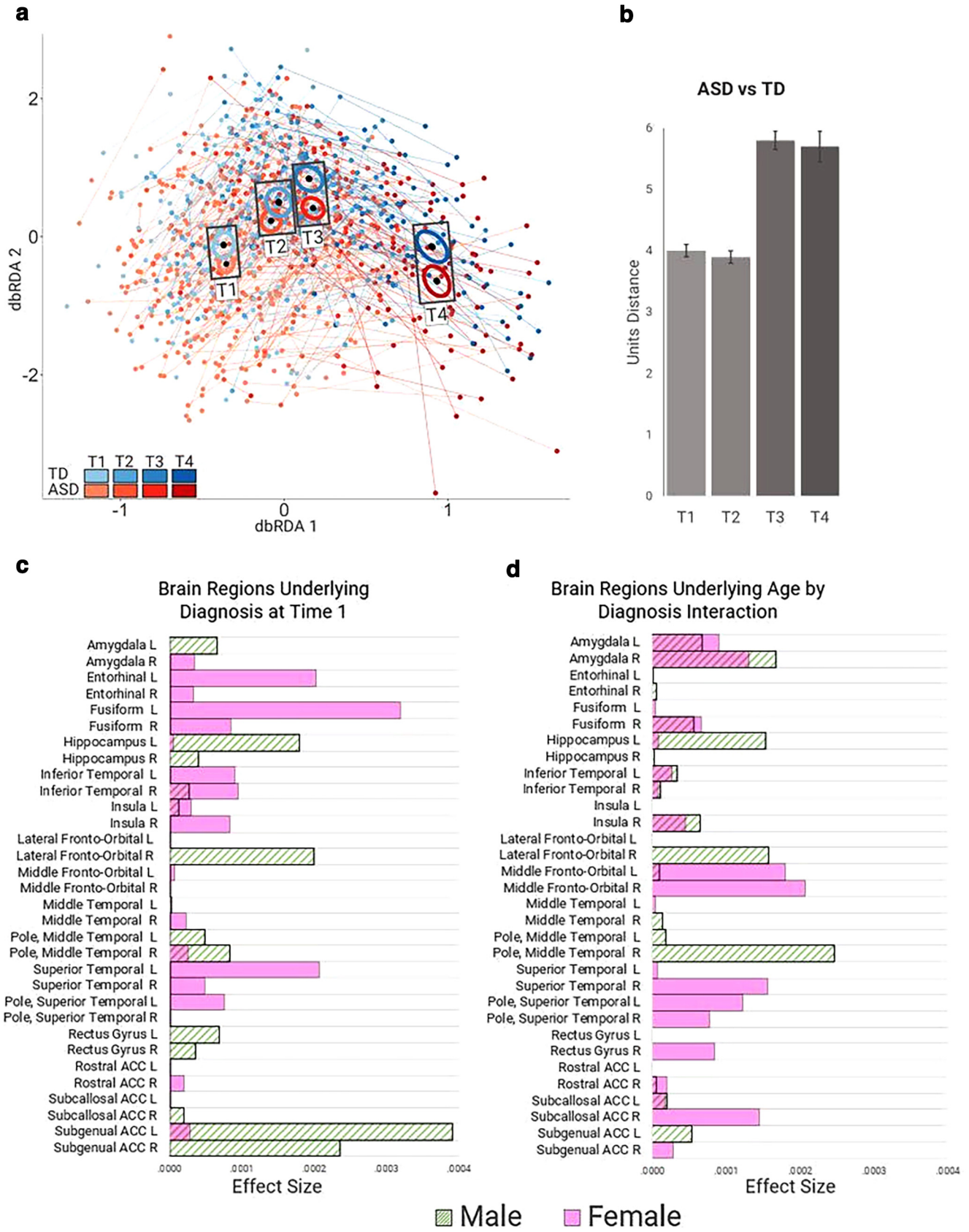

Figure 2. Altered development of amygdala-connected network in autism. MDMR results indicate significantly different development of the amygdala-connected network in autism over time. ***a***, Plot represents the MDMR results using dbRDA, indicating group differences at Time 1, 2, 3, and 4 (T1-T4; mean ages of 38, 52, 64, and 137 months, respectively). dbRDA is a dimension reduction technique that facilitates visualization of relationships in high-dimensional data into two dimensions that capture the most variation. Black dots represent median centroid locations of each group and time point on the first two dbRDA axes. Ellipsoids represent the SE of those group-centroid locations. As apparent from the plots, the first dbRDA axis (horizontal) was highly responsive to participant age over time and exhibited a clear gradient going from younger (left) to older (right). The second dbRDA axis differentiated autism from typical development.

B values ≥ 1.9, *p* values ≤ 0.030). The magnitude of these differences significantly increased in size from early to middle childhood (linear and quadratic age × diagnosis interactions: *B* values ≥ 2.0, *p* values ≤ 0.022) (Fig. 2*a*). This interpretation resulted from increasing distances between autism and TD groups at subsequent time points (Fig. 2*b*). See Model I in Table 2 for regression parameters. Overall, the amygdala-connected network significantly differed between males and females (sex: $B = 3.0$, $p = 0.001$), but two-way (sex × diagnosis) and three-way (sex × diagnosis × age) interactions with sex were not statistically significant (*B* values ≤ 1.2, *p* values ≥ 0.26). Left or right handedness did not significantly moderate the volumetric differences between autistic and TD children (*B* values ≤ 1.4, *p* values ≥ 0.17).

Finally, since all volumes are computed as a proportion of TBV, we conducted an analysis of the development of TBV. Autistic individuals had larger TBV than TD children at T1 ($B = 30$ cm^3, $SE = 9.7$, $t = 3.09$, $p = 0.002$); however, the curvature of the TBV trajectory did not significantly differ by diagnosis, or sex × diagnosis interaction (*B* values ≤ 11, *p* values ≥ 0.34), largely consistent with our prior report (Lee et al., 2020b). These trajectories are plotted in Figure 3.

Comparison of regional differences within amygdala-connected networks across diagnosis, sex, and age

We next examined the contributions of individual brain regions using multivariate effect size analysis, which identifies brain regions that contributed the most to significant effects observed in the MDMR analysis. Specifically, we probed two related questions: (1) How similar were the sets of brain regions that differentiated autism and TD in males and in females? (2) Which brain regions contributed most to the effects of diagnosis in males and females?

We found that the effect sizes that differentiated autism from TD children at T1 were largely dissimilar between males and females, exhibiting little overlap in regional effect sizes (DSC = 0.073). While autism in males at T1 was disproportionately associated with volumetric differences in left subgenual, ACC, right subgenual ACC, and right lateral fronto-orbital gyrus, the greatest differences between autistic and TD females were in the left fusiform gyrus, left superior temporal gyrus, and left entorhinal cortex (Fig. 2*c*). The developmental trajectories of these regions are included in Figure 3.

The sets of brain regions underlying the increasing differences between autism and TD groups from early to middle childhood were also differentiated in males and females, exhibiting moderate agreement or overlap (DSC = 0.294). In males, this developmental effect was disproportionately associated with the right middle temporal pole, right amygdala, right lateral orbital frontal gyrus, and left hippocampus, while in females it was disproportionately associated with the bilateral middle orbitofrontal gyrus, right superior temporal gyrus, and right subcallosal ACC (Fig. 2*d*). The developmental trajectories of these regions are included in Figure 3.

Table 2. Fixed effects from two mixed-level MDMR models predicting volumes of amygdala-connected regions[a]

Model	Effect	Statistic	*p*
I	(Intercept)	28.1	<0.0001
	Sex	2.99	0.001
	Diagnosis	1.89	0.033
	Age	91.5	<0.0001
	Age^2	31.6	<0.0001
	Age × diagnosis	2.02	0.022
	Age^2 × diagnosis	2.27	0.010
II	(Intercept)	7.05	<0.0001
	Sex	3.42	0.0004
	DQ at T1	0.86	0.58
	SRS$^-$	0.38	0.98
	SRS$^+$	0.77	0.68
	Age	63.9	<0.0001
	Age^2	27.0	<0.001
	SRS$^-$ × age	1.35	0.17
	SRS$^-$ × age^2	1.57	0.09
	SRS$^+$ age	2.46	0.006
	SRS$^+$ age^2	3.23	0.0007

[a]Model I: Age is lefted at the mean age of Time 1 (~37 months). Birth sex is effects coded (–0.5 male, 0.5 female). Autism spectrum disorder is the reference diagnostic group in regression. Model II: SRS$^-$: Autistic individuals with SRS scores at Time 1 ≤ 75. SRS$^+$: SRS at Time 1 > 75. TD children served as reference group. Biological sex is effects coded (–0.5 male, 0.5 female). Age is lefted at the mean age of Time 1 (~37 months). DQ at Time 1 was used as a covariate and was lefted at 70. Similar results are observed without controlling for differences in DQ.

Social impairments in early childhood and amygdala-connected development

Consistent with greater autism traits being associated with greater differences in the development of the amygdala-connected network, T1 SRS scores were found to significantly moderate developmental trajectories of the amygdala-connected network between groups (group × age: *B* values ≥ 3.3, *p* values ≤ 0.025) (Fig. 4*a*). The differences between SRS$^+$ and TD groups became significantly larger over time (SRS$^+$ vs TD × age: *B* values ≥ 2.4, *p* values ≤ 0.006), while the trajectories of SRS$^-$ and TD groups did not (SRS$^-$ vs TD × age: *B* values ≤ 1.6, *p* values ≥ 0.09). The trajectories of SRS$^+$ and SRS$^-$ groups diverged quadratically (i.e., with different curvature) (SRS$^+$ vs SRS$^-$ × age^2: *B* values = 2.4, $p = 0.008$), with increasing differences over time (Fig. 4*b*). For model parameters, see Model II in Table 2. No sex × group interactions were significant at any time point (*B* values ≤ 2.3, *p* values ≥ 0.28).

Examination of regional effect sizes in males and females separately suggests both similarities and differences between sexes. Contrasting the SRS$^+$ with TD at T1 revealed low to moderate overlap (DSC = 0.285), with differences in males being disproportionately associated with left subgenual ACC and right lateral orbitofrontal gyrus, and in females, with right amygdala, and bilateral gyrus rectus. Male and female effect sizes associated with the longitudinal increase in the differences between SRS$^+$ and TD groups exhibited moderate agreement (DSC = 0.473), with differences in males being disproportionately associated with right middle temporal gyrus and right amygdala, and differences in females associated with right amygdala and right subgenual ACC.

Specificity of effects related to the amygdala-connected network

To test the specificity of the above findings to the amygdala-connected network, we conducted longitudinal MDMR analyses on

←

Together, the graph represents diverging trajectories of development in autism. ***b***, Bar plot of the computed distances between autism and typically developing groups by time point, showing that differences became greater as participants aged. ***c***, Effect size analysis of the effect of diagnosis revealed minimal overlap when separated by biological sex. ***d***, Effect size analysis of the effect of the age × diagnosis interaction also revealed minimal overlap when separated by biological sex.

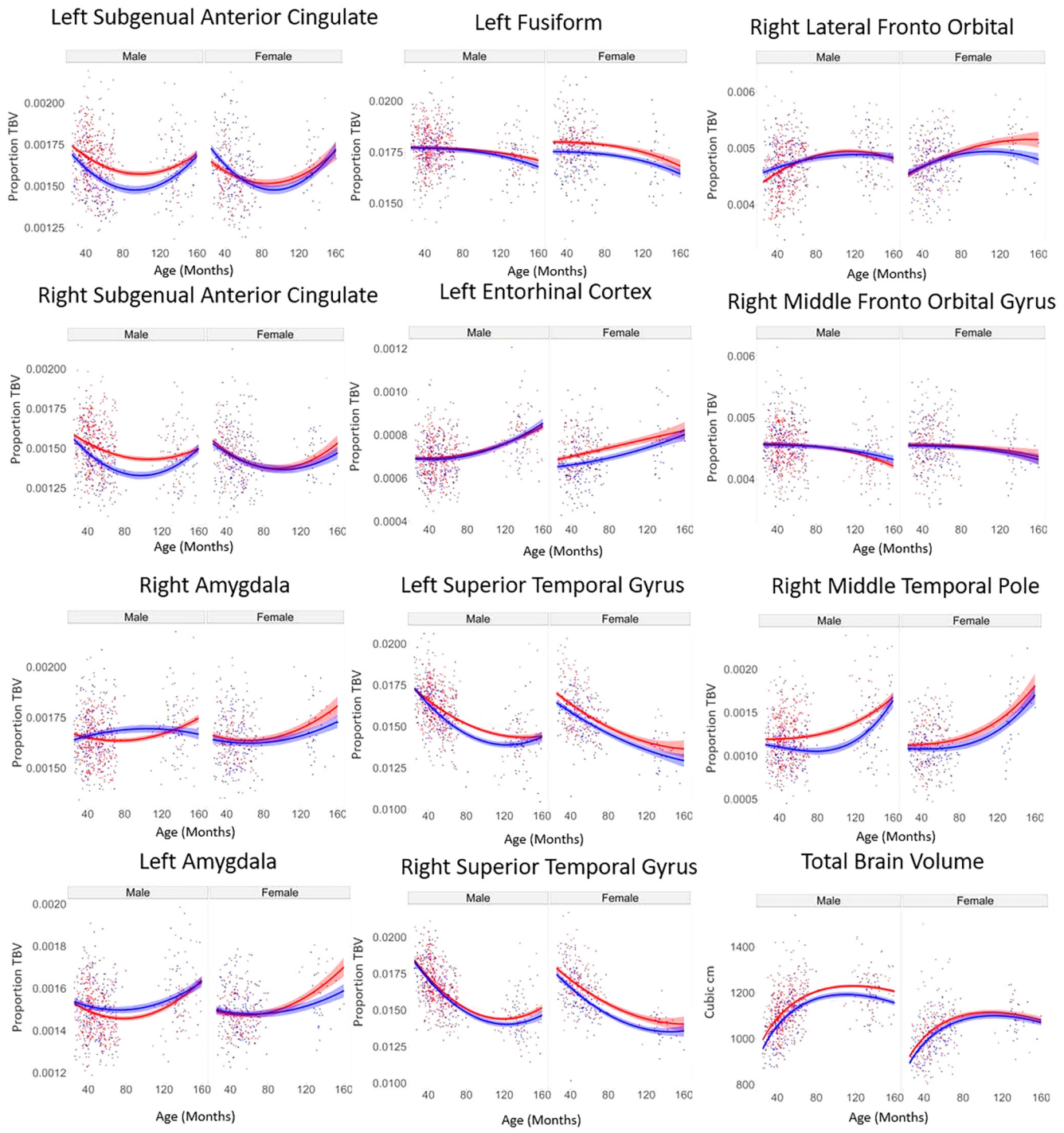

Figure 3. Longitudinal trajectories of regions within the amygdala-connected network. Volumetric trajectories for brain regions exhibiting the top two or three effect sizes in the MDMR analyses. The effects of diagnosis at Time 1 (age ~38 months) were largest in left and right subgenual ACC and right lateral fronto-orbital gyrus in males, and left entorhinal, left fusiform, and left superior temporal gyrus in females. The effects of diagnosis that changed most with age were plotted for the right pole of the middle temporal gyrus, right lateral fronto-orbital cortex, and right amygdala in males, and plotted for the right middle fronto-orbital cortex, right superior temporal gyrus, and right amygdala in females. The trajectories of left amygdala and of TBV development are also plotted.

a set of cortical gray matter ROIs that are not monosynaptically connected with the amygdala. In these analyses, there were no significant effects of diagnosis or significant interactions with diagnosis (see Table 3, Model I). There were also no significant differences between the TD, SRS^{-}, and SRS^{+} group trajectories (see Table 3, Model II). We also compared effect sizes between amygdala-connected ROIs and non–amygdala-connected ROIs for the effect of diagnosis at Time 1. The mean effect size was 2.7 times larger in the amygdala-connected network than in the non–amygdala-connected cortical ROIs. Finally, we summed the volumes of all regions within each set of ROIs and conducted a univariate mixed effects model examining the effects of diagnosis between amygdala-connected network and the non–amygdala-connected cortical regions after controlling for linear and quadratic age terms. We observed a significant interaction between diagnosis and ROI set ($B = 0.0027$, SE = 0.0009, $t = 2.95$, $p = 0.003$),

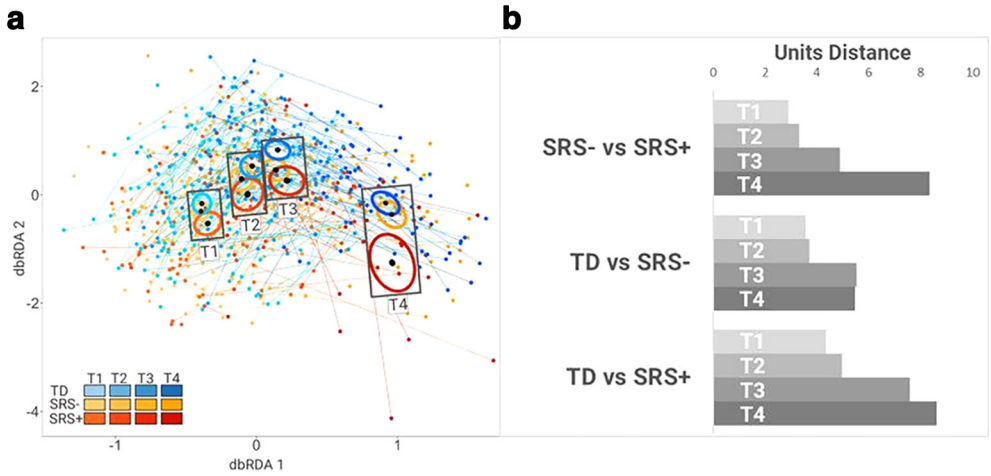

Figure 4. Altered development of the amygdalocentric network in autism with higher SRS T scores at Time 1. ***a***, Plot represent development of the amygdalocentric profile using dbRDA, indicating group differences at Time 1, 2, 3, and 4 (T1-T4; mean ages of 38, 52, 64, and 137 months, respectively) in autistic children with higher (SRS^+) and lower (SRS^-) Time 1 SRS T scores and TD children. Black dots represent median centroid locations of SRS^+, SRS^-, and TD groups at each time point on the first two dbRDA axes. Ellipsoids represent the SE of those group-centroid locations. Plots represent diverging developmental trajectories between TD and SRS^+, but not SRS^- groups. ***b***, Bar plot of the computed distances between SRS^+, SRS^-, and TD groups at each time point. Distances confirm pattern of increasing separation over time between TD and the SRS^+ group that has more impacted social functioning.

Table 3. Analysis of cortical brain region without monosynaptic connection with the amygdala[a]

Model	Effect	Statistic	*p*
I	(Intercept)	68.9	<0.0001
	Sex	3.13	0.0003
	Diagnosis	0.78	0.72
	Age	92.3	<0.0001
	Age^2	36.3	<0.0001
	Age × diagnosis	0.60	0.92
	Age^2 × diagnosis	0.61	0.91
II	(Intercept)	13.9	<0.0001
	Sex	3.02	0.0005
	DQ at T1	1.2	0.25
	SRS^-	1.0	0.37
	SRS^+	0.99	0.44
	Age	54.9	<0.0001
	Age^2	25.2	<0.0001
	SRS^- × age	0.68	0.83
	SRS^- × age^2	0.62	0.89
	SRS^+ age	1.1	0.35
	SRS^+ age^2	1.4	0.12

[a]Model I: Age is lefted at the mean age of Time 1 (~37 months). Birth sex is effects coded (–0.5 male, 0.5 female). Autism spectrum disorder is the reference diagnostic group in regression. Model II: SRS^-: Autistic individuals with SRS scores at Time 1 ≤ 75. SRS^+: SRS at Time 1 > 75. TD children served as reference group. Biological sex is effects coded (–0.5 male, 0.5 female). Age is lefted at the mean age of Time 1 (~37 months). DQ at Time 1 was used as a covariate and was lefted at 70. Similar results are observed without controlling for differences in DQ.

such that the volume of amygdala-connected network was significantly larger in autism, but not in cortex not monosynaptically connected to the amygdala (see Fig. 5).

Discussion

The amygdala acts as the central hub of a brain network that is involved in socioemotional functioning and exhibits pervasive alterations in autism (Freese and Amaral, 2009; Bickart et al., 2014; Mears and Pollard, 2016; Hennessey et al., 2018). Here we examined the global pattern of volumetric change in a network of brain regions sharing monosynaptic connections with the amygdala. We report structural alterations in this amygdala network in autism that grow larger from early to middle childhood, particularly in those with more affected social functioning. The results of this study reinforce the idea that brain development relevant to social cognition and the neurobiology of autism does not end in infancy and that childhood is still a period amenable to intervention (Estes et al., 2015).

The divergence between autistic and TD children was most prevalent in those with greater social communication problems in early childhood (i.e., higher SRS scores). The strength of this relationship became more robust over time, suggesting a cascading effect from earlier social behaviors to later brain maturation. There is precedent for behavioral measurements serving as leading indicators of subsequent brain development. For example, a well-powered population-based study reported that baseline internalizing and externalizing problems predicted changes in subcortical brain volume, but not vice versa (Muetzel et al., 2018). The relative concurrency brain–behavior relationships in autism will be a fertile area for future research.

Diagnostic differences were of comparable magnitude across males and females. This result stands in contrast to our prior MDMR analysis of amygdala resting-state functional connectivity in a subset of these participants (Lee et al., 2020a). There we reported attenuated sex differences in autism, but not TD, consistent with the gender incoherence hypothesis (Bejerot et al., 2012); it is unclear whether this discrepancy results from differences in imaging modality or some other factor. Nevertheless, qualitative differences by sex were evident.

In males at 38 months (mean age at baseline), bilateral subgenual ACC was most affected in autism. The subgenual ACC is densely innervated by the basal and accessory basal nuclei of the amygdala, forming a circuit subserving emotion regulation and fear extinction (Amaral and Price, 1984; Amaral, 2002; Sharma et al., 2020). The subgenual ACC monitors and signals social prediction error, which is the concordance between the expected behaviors and actual behaviors of others (Apps et al., 2016). The subgenual ACC also subserves anxiety functioning by initiating avoidance behaviors and emotion regulation (Chavanne and Robinson, 2021).

In contrast, autistic females at 38 months predominately exhibited alterations in the left superior temporal gyrus. Amygdala connections with the superior temporal gyrus are

implicated in disruptions to social perception and communication (Abrams et al., 2019), and are widely implicated in anxiety disorders (Xia et al., 2017). Altered superior temporal gyrus volumes have previously been associated with common variants of the autism-related gene CNTNAP2, a gene also implicated in social interaction, communication behaviors, as well as social anxiety in autism (Stein et al., 2012; Li et al., 2021). We note that the left lateralization of left superior temporal gyrus in girls runs counter to the frequently reported right lateralization of temporal lobe differences in autism, especially in association with language function (see, e.g., Kleinhans et al., 2008). However, few studies have examined whether atypical laterality in autism is consistent across sex (Floris et al., 2021). Moreover, brain lateralization emerges across childhood (Olulade et al., 2020; Floris et al., 2021). Consistent with this developmental perspective, right lateralized group differences in superior temporal gyrus in females and middle temporal gyrus in males increased over development.

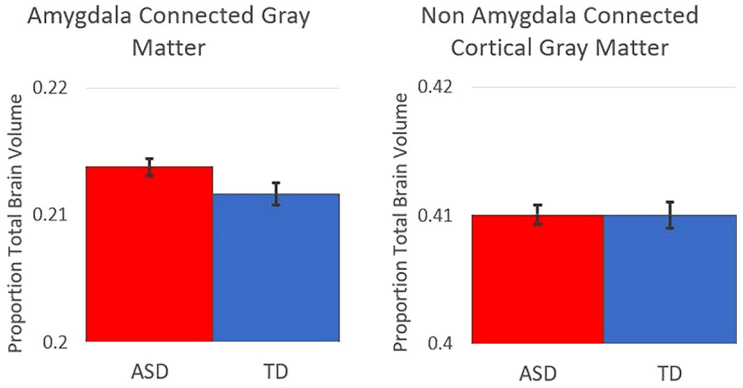

Figure 5. Volumes of amygdala-connected network and non–amygdala-connected cortical regions. Autism is associated with increased total volume (adjusted by total brain volume) of gray matter regions with monosynaptic amygdala connections, but not with gray matter regions without monosynaptic connections with the amygdala. Error bars indicate 95% confidence intervals.

At 38 months of age (mean age at baseline), the amygdala itself was not particularly distinguishing of autism, although figuring somewhat more prominently in changes over time. The amygdala is hypothesized to undergo a period of heightened growth in autism; however, the majority of that overgrowth may occur in infancy and end sometime in childhood (Avino et al., 2018; Xu et al., 2020; Shen et al., 2022). The exact timing of the transition from accelerated to slowed amygdala growth remains uncertain, however; and substantial disagreement exists between the available studies. Methodological differences and heterogeneity in co-occurring conditions, such as anxiety, likely contribute to the inconsistency of findings. For example, we recently compared amygdala growth (Andrews et al., 2022) in individuals with traditional forms of anxiety, as defined in the Diagnostic and Statistical Manual of Mental Disorders (DSM), with those with a form of anxiety distinctly related to autism, which was assessed by the Anxiety Disorders Interview Schedule–Autism Addendum (Kerns et al., 2017). In this study, autistic children with DSM anxiety tended to have persistent amygdala overgrowth, whereas those with autism-distinct anxieties had significantly slower right amygdala growth compared with other autistic and TD children. Future research should examine how autism-distinct and DSM forms of anxiety might shape development of the amygdala-connected network.

Broadly, the current results provide support for a growing literature that has identified qualitatively different neurobiological alterations in males and females with autism (Lai et al., 2015; Hammill et al., 2021). For example, brain morphometry associated with autism was recently reported to differ qualitatively in males and females, even while the overall quantitative size of the effects did not (Hammill et al., 2021). We note that qualitatively distinct alterations in autistic males and females do not necessarily indicate different etiologies. This is simply because those alterations are measured against different baselines: their sex-specific TD peers. This may be especially relevant because sex differences are observed across multiple levels of analysis (McCarthy and Arnold, 2011) and because the etiology of autism is intricately linked to biological sex (Alaerts et al., 2016; Lai et al., 2017), and to the full spectrum of gender-variant identities (Strang et al., 2014).

The present research benefits by using a person-centric, multivariate methodology that differs from predominate approaches in volumetric MRI studies. which either examine a single ROI or conduct brain-wide mass-univariate analyses. In contrast, we examined the confluence of volumetric differences across an anatomically grounded, amygdala-connected brain network using a robust multivariate approach, efficiently aggregating evidence across ROIs that individually often provide only weak or nonsignificant evidence for systematic differences. We complemented the prior approach with a bootstrap analysis of effect sizes to estimate the relative contribution of each brain region to the overall multivariate pattern. This combined approach allows us to assess both quantitative and qualitative differences in the effects of autism (Lai et al., 2017; Hammill et al., 2021). These data also highlight the importance of longitudinal research. Cross-sectional investigations of volumetric development are comparatively disadvantaged from the substantial interindividual variability in volumes. In contrast, in longitudinal research, participants serve as their own matched control, effectively increasing the observed developmental signal. Despite its strengths, the current research faces several limitations. First, a consequence of exclusively examining regions with monosynaptic connection, we preclude brain regions that are influenced through polysynaptic pathways. While overall, there is overall strong correspondence between the regions we examined and meta-analytic maps of amygdala resting-state functional connectivity (https://neurosynth.org) (de la Vega et al., 2016), one cortical region of particular note that was excluded in the present analysis was the posterior cingulate cortex (PCC). While the PCC is not monosynaptically connected with the amygdala (Kobayashi and Amaral, 2003, 2007), it frequently exhibits functional correlations with the amygdala. The PCC is an important brain region in the default mode network that is altered in autism (Padmanabhan et al., 2017). Nevertheless, in our examination of ROIs outside of the amygdala-connected network, the PCC did not reliably exhibit an effect size >0, suggesting minimal diagnostic differences. Ultimately, we believe that the advantages of increasing the specificity of included brain regions was worth the potential cost of excluding contributing, yet tertiary brain regions. Another potential limitation of this research was its reliance on ROI volumetric data. Voxel-wise approaches may uncover differences obscured by larger ROIs. However, ROIs offered several advantages, including accessible boundaries that enabled us to examine our *a priori* hypotheses. Relatedly, another limitation of this research is that the amygdala is treated as a single unit, despite it having multiple

subnuclei with unique monosynaptic connections. Unfortunately, the subnuclei are not discernable in standard MRI, and the existing techniques (e.g., FreeSurfer) (Saygin et al., 2017) wholly depend on the dubious validity of statistical relationships developed on nonautistic, nonpediatric populations (Wisse et al., 2014, 2021; Seiger et al., 2021). Finally, although we included more autistic females than many other studies, a sex imbalance remained, potentially limiting statistical power to find smaller and interactive effects.

In conclusion, this research sought to examine the structural development of a network of brain regions with monosynaptic connection to the amygdala in autistic and typical development. We found global differences that increase with age, which were associated with early social communication problems. We also discovered qualitative differences between males and females in terms of which brain regions within the amygdala-connected network exhibited differences in autism compared with sex-matched controls. These results indicate ongoing alterations to brain development relevant to autism and social functioning, the impact of which may be to suggest potential targets for future clinical interventions.

References

Abrams DA, Padmanabhan A, Chen T, Odriozola P, Baker AE, Kochalka J, Phillips JM, Menon V (2019) Impaired voice processing in reward and salience circuits predicts social communication in children with autism. Elife 8:e39906.

Aggarwal CC, Hinneburg A, Keim DA (2001) On the surprising behavior of distance metrics in high dimensional space. In International conference on database theory, pp 420–434. Springer, Berlin, Heidelberg.

Alaerts K, Swinnen SP, Wenderoth N (2016) Sex differences in autism: a resting-state fMRI investigation of functional brain connectivity in males and females. Soc Cogn Affect Neurosci 11:1002–1016.

Amaral DG (2002) The primate amygdala and the neurobiology of social behavior: implications for understanding social anxiety. Biol Psychiatry 51:11–17.

Amaral DG, Price JL (1984) Amygdalo-cortical projections in the monkey (*Macaca fascicularis*). J Comp Neurol 230:465–496.

Anderson MJ, Willis TJ (2003) Canonical analysis of principal coordinates: a useful method of constrained ordination for ecology. Ecology 84:511–525.

Andrews DS, Aksman L, Kerns CM, Lee JK, Winder-Patel BM, Harvey DJ, Waizbard-Bartov E, Heath B, Solomon M, Rogers SJ, Altmann A, Nordahl CW, Amaral DG (2022) Association of amygdala development with different forms of anxiety in autism spectrum disorder. Biol Psychiatry 91:977–987.

Anon (2013) Diagnostic and statistical manual of mental disorders, Ed 5. Arlington: American Psychiatric Association.

Apostol TM, Mnatsakanian MA (2003) Sums of squares of distances in m-space. Am Math Mthly 110:516–526.

Apps MA, Rushworth MF, Chang SW (2016) The anterior cingulate gyrus and social cognition: tracking the motivation of others. Neuron 90:692–707.

Avino TA, Barger N, Vargas MV, Carlson EL, Amaral DG, Bauman MD, Schumann CM (2018) Neuron numbers increase in the human amygdala from birth to adulthood, but not in autism. Proc Natl Acad Sci USA 115:3710–3715.

Bejerot S, Eriksson JM, Bonde S, Carlström K, Humble MB, Eriksson E (2012) The extreme male brain revisited: gender coherence in adults with autism spectrum disorder. Br J Psychiatry 201:116–123.

Benjamini Y, Hochberg Y (1995) Controlling the false discovery rate: a practical and powerful approach to multiple testing. J R Stat Soc B (Methodological) 57:289–300.

Bickart KC, Dickerson BC, Barrett LF (2014) The amygdala as a hub in brain networks that support social life. Neuropsychologia 63:235–248.

Carmichael ST, Price JL (1995) Limbic connections of the orbital and medial prefrontal cortex in macaque monkeys. J Comp Neurol 363:615–641.

Ceritoglu C, Oishi K, Li X, Chou MC, Younes L, Albert M, Lyketsos C, van Zijl PC, Miller MI, Mori S (2009) Multi-contrast large deformation diffeomorphic metric mapping for diffusion tensor imaging. Neuroimage 47:618–627.

Chavanne AV, Robinson OJ (2021) The overlapping neurobiology of induced and pathological anxiety: a meta-analysis of functional neural activation. Am J Psychiatry 178:156–164.

Constantino JN, Gruber CP (2012) Social responsiveness scale: SRS-2. Torrance, CA: Western Psychological Services.

de la Vega A, Chang LJ, Banich MT, Wager TD, Yarkoni T (2016) Large-scale meta-analysis of human medial frontal cortex reveals tripartite functional organization. J Neurosci 36:6553–6562.

Dice LR (1945) Measures of the amount of ecologic association between species. Ecology 26:297–302.

Estes A, Munson J, Rogers SJ, Greenson J, Winter J, Dawson G (2015) Long-term outcomes of early intervention in 6-year-old children with autism spectrum disorder. J Am Acad Child Adolesc Psychiatry 54:580–587.

Fadok JP, Markovic M, Tovote P, Lüthi A (2018) New perspectives on central amygdala function. Curr Opin Neurobiol 49:141–147.

Floris DL, et al. (2021) Atypical brain asymmetry in autism: a candidate for clinically meaningful stratification. Biol Psychiatry Cogn Neurosci Neuroimaging 6:802–812.

Freese JL, Amaral DG (2009) Neuroanatomy of the primate amygdala. In: The human amygdala, pp 3–42. New York: Guilford.

Gangopadhyay P, Chawla M, Dal Monte O, Chang SW (2021) Prefrontal–amygdala circuits in social decision-making. Nat Neurosci 24:5–18.

Gotham K, Pickles A, Lord C (2009) Standardizing ADOS scores for a measure of severity in autism spectrum disorders. J Autism Dev Disord 39:693–705.

Gower JC (1966) Some distance properties of latent root and vector methods used in multivariate analysis. Biometrika 53:325–338.

Hammill C, Lerch JP, Taylor MJ, Ameis SH, Chakravarty MM, Szatmari P, Anagnostou E, Lai MC (2021) Quantitative and qualitative sex modulations in the brain anatomy of autism. Biol Psychiatry Cogn Neurosci Neuroimaging 6:898–909.

Hennessey T, Andari E, Rainnie DG (2018) RDoC-based categorization of amygdala functions and its implications in autism. Neurosci Biobehav Rev 90:115–129.

Hoffman L (2015) Longitudinal analysis: modeling within-person fluctuation and change. Milton Park, UK: Routledge.

Hori Y, Schaeffer DJ, Gilbert KM, Hayrynen LK, Cléry JC, Gati JS, Menon RS, Everling S (2020) Comparison of resting-state functional connectivity in marmosets with tracer-based cellular connectivity. Neuroimage 204:116241.

Insausti R, Amaral DG, Cowan WM (1987) The entorhinal cortex of the monkey: III. Subcortical afferents. J Comp Neurol 264:396–408.

Kerns CM, Renno P, Kendall PC, Wood JJ, Storch EA (2017) Anxiety disorders interview schedule–autism addendum: reliability and validity in children with autism spectrum disorder. J Clin Child Adolesc Psychol 46:88–100.

Kleinhans NM, Müller RA, Cohen DN, Courchesne E (2008) Atypical functional lateralization of language in autism spectrum disorders. Brain Res 1221:115–125.

Kobayashi Y, Amaral DG (2003) Macaque monkey retrosplenial cortex: II. Cortical afferents. J Comp Neurol 466:48–79.

Kobayashi Y, Amaral DG (2007) Macaque monkey retrosplenial cortex: III. Cortical efferents. J Comp Neurol 502:810–833.

Lai MC, Lombardo MV, Auyeung B, Chakrabarti B, Baron-Cohen S (2015) Sex/gender differences and autism: setting the scene for future research. J Am Acad Child Adolesc Psychiatry 54:11–24.

Lai MC, Lerch JP, Floris DL, Ruigrok AN, Pohl A, Lombardo MV, Baron-Cohen S (2017) Imaging sex/gender and autism in the brain: etiological implications. J Neurosci Res 95:380–397.

Lee JK, Amaral DG, Solomon M, Rogers SJ, Ozonoff S, Nordahl CW (2020a) Sex differences in the amygdala resting-state connectome of children with autism spectrum disorder. Biol Psychiatry Cogn Neurosci Neuroimaging 5:320–329.

Lee JK, Andrews DS, Ozonoff S, Solomon M, Rogers S, Amaral DG, Nordahl CW (2020b) Longitudinal evaluation of cerebral growth across childhood in boys and girls with autism spectrum disorder. Biol Psychiatry 90:286–294.

Legendre P, Anderson MJ (1999) Distance-based redundancy analysis: testing multispecies responses in multifactorial ecological experiments. Ecol Monogr 69:1–24.

Li D, Zhang L, Bai T, Huang W, Ji GJ, Yang T, Zhang Y, Tian Y, Qiu B, Wang K (2021) Common variants of the autism-associated CNTNAP2 gene contribute to the modulatory effect of social function mediated by temporal cortex. Behav Brain Res 409:113319.

Long J, Ryoo J (2010) Using fractional polynomials to model non-linear trends in longitudinal data. Br J Math Stat Psychol 63:177–203.

Lord C, Rutter M, Le Couteur A (1994) Autism Diagnostic Interview-Revised: a revised version of a diagnostic interview for caregivers of individuals with possible pervasive developmental disorders. J Autism Dev Disord 24:659–685.

Lord C, Risi S, Lambrecht L, Cook EH, Leventhal BL, DiLavore PC, Pickles A, Rutter M (2000) The Autism Diagnostic Observation Schedule–Generic: a standard measure of social and communication deficits associated with the spectrum of autism. 30:205–223.

Lord C, Rutter M, DiLavore PC, Risi, Gotham K, Bishop S (2012) Autism diagnostic observation schedule, Ed 2. Torrance, CA: Western Psychological Services.

McArtor DB, Lubke GH, Bergeman CS (2017) Extending multivariate distance matrix regression with an effect size measure and the asymptotic null distribution of the test statistic. Psychometrika 82:1052–1077.

McCarthy MM, Arnold AP (2011) Reframing sexual differentiation of the brain. Nat Neurosci 14:677–683.

Mears D, Pollard HB (2016) Network science and the human brain: using graph theory to understand the brain and one of its hubs, the amygdala, in health and disease. J Neurosci Res 94:590–605.

Morgan JT, Barger N, Amaral DG, Schumann CM (2014) Stereological study of amygdala glial populations in adolescents and adults with autism spectrum disorder. PLoS One 9:e110356.

Mori S, Wu D, Ceritoglu C, Li Y, Kolasny A, Vaillant MA, Faria AV, Oishi K, Miller MI (2016) MRICloud: delivering high-throughput MRI neuroinformatics as cloud-based software as a service. Comput Sci Eng 18:21–35.

Mosconi MW, Cody-Hazlett H, Poe MD, Gerig G, Gimpel-Smith R, Piven J (2009) Longitudinal study of amygdala volume and joint attention in 2- to 4-year-old children with autism. Arch Gen Psychiatry 66:509–516.

Muetzel RL, Blanken LM, van der Ende J, El Marroun H, Shaw P, Sudre G, van der Lugt A, Jaddoe VW, Verhulst FC, Tiemeier H, White T (2018) Tracking brain development and dimensional psychiatric symptoms in children: a longitudinal population-based neuroimaging study. Am J Psychiatry 175:54–62.

Mullen EM (1995) Mullen scales of early learning. Circle Pines, MN: AGS.

Müller RA, Fishman I (2018) Brain connectivity and neuroimaging of social networks in autism. Trends Cogn Sci 22:1103–1116.

Mundy P (2018) A review of joint attention and social-cognitive brain systems in typical development and autism spectrum disorder. Eur J Neurosci 47:497–514.

Munson J, Dawson G, Abbott R, Faja S, Webb SJ, Friedman SD, Shaw D, Artru A, Dager SR (2006) Amygdalar volume and behavioral development in autism. Arch Gen Psychiatry 63:686–693.

Nordahl CW, Simon TJ, Zierhut C, Solomon M, Rogers SJ, Amaral DG (2008) Brief report: methods for acquiring structural MRI data in very young children with autism without the use of sedation. J Autism Dev Disord 38:1581–1590.

Nordahl CW, Scholz R, Yang X, Buonocore MH, Simon T, Rogers S, Amaral DG (2012) Increased rate of amygdala growth in children aged 2 to 4 years with autism spectrum disorders: a longitudinal study. Arch Gen Psychiatry 69:53–61.

Nordahl CW, Mello M, Shen AM, Shen MD, Vismara LA, Li D, Harrington K, Tanase C, Goodlin-Jones B, Rogers S, Abbeduto L, Amaral DG (2016) Methods for acquiring MRI data in children with autism spectrum disorder and intellectual impairment without the use of sedation. J Neurodev Disord 8:20.

Nordahl CW, Iosif AM, Young GS, Hechtman A, Heath B, Lee JK, Libero L, Reinhardt VP, Winder-Patel B, Amaral DG, Rogers S, Solomon M, Ozonoff S (2020) High psychopathology subgroup in young children with autism: associations with biological sex and amygdala volume. J Am Acad Child Adolesc Psychiatry 59:1353–1363.e2.

Oishi K, Faria A, Jiang H, Li X, Akhter K, Zhang J, Hsu JT, Miller MI, van Zijl PC, Albert M, Lyketsos CG, Woods R, Toga AW, Pike GB, Rosa-Neto P, Evans A, Mazziotta J, Mori S (2009) Atlas-based whole brain white matter analysis using large deformation diffeomorphic metric mapping: application to normal elderly and Alzheimer's disease participants. Neuroimage 46:486–499.

Olulade OA, Seydell-Greenwald A, Chambers CE, Turkeltaub PE, Dromerick AW, Berl MM, Gaillard WD, Newport EL (2020) The neural basis of language development: changes in lateralization over age. Proc Natl Acad Sci USA 117:23477–23483.

Padmanabhan A, Lynch CJ, Schaer M, Menon V (2017) The default mode network in autism. Biol Psychiatry Cogn Neurosci Neuroimaging 2:476–486.

Reinhardt VP, Iosif AM, Libero L, Heath B, Rogers SJ, Ferrer E, Nordahl C, Ghetti S, Amaral D, Solomon M (2020) Understanding hippocampal development in young children with autism spectrum disorder. J Am Acad Child Adolesc Psychiatry 59:1069–1079.

Ritchie SJ, Cox SR, Shen X, Lombardo MV, Reus LM, Alloza C, Harris MA, Alderson HL, Hunter S, Neilson E, Liewald DC, Auyeung B, Whalley HC, Lawrie SM, Gale CR, Bastin ME, McIntosh AM, Deary IJ (2018) Sex differences in the adult human brain: evidence from 5216 UK Biobank participants. Cereb Cortex 28:2959–2975.

Russchen FT, Bakst I, Amaral DG, Price JL (1985) The amygdalostriatal projections in the monkey: an anterograde tracing study. Brain Res 329:241–257.

Rutishauser U, Tudusciuc O, Wang S, Mamelak AN, Ross IB, Adolphs R (2013) Single-neuron correlates of atypical face processing in autism. Neuron 80:887–899.

Rutter M, Bailey A, Lord C (2003) SCQ. The Social Communication Questionnaire. Torrance, CA: Western Psychological Services.

Satterthwaite TD, Wolf DH, Roalf DR, Ruparel K, Erus G, Vandekar S, Gennatas ED, Elliott MA, Smith A, Hakonarson H, Verma R, Davatzikos C, Gur RE, Gur RC (2015) Linked sex differences in cognition and functional connectivity in youth. Cereb Cortex 25:2383–2394.

Saunders RC, Rosene DL, Van Hoesen GW (1988) Comparison of the efferents of the amygdala and the hippocampal formation in the rhesus monkey: II. Reciprocal and non-reciprocal connections. J Comp Neurol 271:185–207.

Saygin ZM, Kliemann D, Iglesias JE, van der Kouwe AJ, Boyd E, Reuter M, Stevens A, Van Leemput K, McKee A, Frosch MP, Fischl B, Augustinack JC, Alzheimer's Disease Neuroimaging Initiative (2017) High-resolution magnetic resonance imaging reveals nuclei of the human amygdala: manual segmentation to automatic atlas. Neuroimage 155:370–382.

Schumann CM, Amaral DG (2006) Stereological analysis of amygdala neuron number in autism. J Neurosci 26:7674–7679.

Schumann CM, Hamstra J, Goodlin-Jones BL, Lotspeich LJ, Kwon H, Buonocore MH, Lammers CR, Reiss AL, Amaral DG (2004) The amygdala is enlarged in children but not adolescents with autism; the hippocampus is enlarged at all ages. J Neurosci 24:6392–6401.

Schumann CM, Barnes CC, Lord C, Courchesne E (2009) Amygdala enlargement in toddlers with autism related to severity of social and communication impairments. Biol Psychiatry 66:942–949.

Seiger R, Hammerle FP, Godbersen GM, Reed MB, Spurny-Dworak B, Handschuh P, Klöbl M, Unterholzner J, Gryglewski G, Vanicek T, Lanzenberger R (2021) Comparison and reliability of hippocampal subfield segmentations within FreeSurfer utilizing T1- and T2-weighted multispectral MRI data. Front Neurosci 15:666000.

Sharma KK, Kelly EA, Pfeifer CW, Fudge JL (2020) Translating fear circuitry: amygdala projections to subgenual and perigenual anterior cingulate in the macaque. Cereb Cortex 30:550–562.

Shattuck DW, Mirza M, Adisetiyo V, Hojatkashani C, Salamon G, Narr KL, Poldrack RA, Bilder RM, Toga AW (2008) Construction of a 3D probabilistic atlas of human cortical structures. Neuroimage 39:1064–1080.

Shen MD, et al., IBIS Network (2022) Subcortical brain development in autism and fragile X syndrome: evidence for dynamic, age- and disorder-specific trajectories in infancy. Am J Psychiatry. doi: 10.1176/appi.ajp.21090896.

Spreen O, Strauss E (1991) A compendium of neuropsychological tests: administration, norms, and commentary. New York: Oxford UP.

Stefanacci L, Amaral DG (2000) Topographic organization of cortical inputs to the lateral nucleus of the macaque monkey amygdala: a retrograde tracing study. J Comp Neurol 421:52–79.

Stefanacci L, Amaral DG (2002) Some observations on cortical inputs to the macaque monkey amygdala: an anterograde tracing study. J Comp Neurol 451:301–323.

Stefanacci L, Suzuki WA, Amaral DG (1996) Organization of connections between the amygdaloid complex and the perirhinal and parahippocampal cortices in macaque monkeys. J Comp Neurol 375:552–582.

Stein JL, et al., Enhancing Neuro Imaging Genetics through Meta-Analysis Consortium (2012) Identification of common variants associated with human hippocampal and intracranial volumes. Nat Genet 44:552–561.

Strang JF, Kenworthy L, Dominska A, Sokoloff J, Kenealy LE, Berl M, Walsh K, Menvielle E, Slesaransky-Poe G, Kim KE, Luong-Tran C, Meagher H, Wallace GL (2014) Increased gender variance in autism spectrum disorders and attention deficit hyperactivity disorder. Arch Sex Behav 43:1525–1533.

Tang X, Oishi K, Faria AV, Hillis AE, Albert MS, Mori S, Miller MI (2013) Bayesian parameter estimation and segmentation in the multi-atlas random orbit model. PLoS One 8:e65591.

Wang H, Yushkevich PA (2013) Multi-atlas segmentation with joint label fusion and corrective learning: an open source implementation. Front Neuroinform 7:27.

Werling DM, Geschwind DH (2013) Sex differences in autism spectrum disorders. Curr Opin Neurol 26:146–153.

Wisse LE, Biessels GJ, Geerlings MI (2014) A critical appraisal of the hippocampal subfield segmentation package in FreeSurfer. Front Aging Neurosci 6:261.

Wisse LE, Chételat G, Daugherty AM, de Flores R, la Joie R, Mueller SG, Stark CE, Wang L, Yushkevich PA, Berron D, Raz N, Bakker A, Olsen RK, Carr VA (2021) Hippocampal subfield volumetry from structural isotropic 1 mm^3 MRI scans: a note of caution. Hum Brain Mapp 42:539–550.

Xia L, Li S, Wang T, Guo Y, Meng L, Feng Y, Cui Y, Wang F, Ma J, Jiang G (2017) Spontaneous alterations of regional brain activity in patients with adult generalized anxiety disorder. Neuropsychiatr Dis Treat 13:1957–1965.

Xu Q, Zuo C, Liao S, Long Y, Wang Y (2020) Abnormal development pattern of the amygdala and hippocampus from childhood to adulthood with autism. J Clin Neurosci 78:327–332.

Zapala MA, Schork NJ (2012) Statistical properties of multivariate distance matrix regression for high-dimensional data analysis. Front Genet 3:190.